

# High Cell Density and Antimicrobial Persistence in *Streptococcus Pyogenes*

**Caroline Martini**

Universidade Federal do Rio de Janeiro, Instituto de Microbiologia Paulo de Góes, RJ, Brazil

**Amada Coronado**

Universidade Federal do Rio de Janeiro, Instituto de Microbiologia Paulo de Góes, RJ, Brazil

**Maria Celeste Melo**

Universidade Federal do Rio Grande do Norte, Natal, RN

**Clarice Gobbi**

Universidade Federal do Rio de Janeiro, Instituto de Microbiologia Paulo de Góes, RJ, Brazil

**Úrsula Lopez**

Universidade Federal do Rio de Janeiro, Instituto de Microbiologia Paulo de Góes, RJ, Brazil

**Marcos Mattos**

Universidade Federal do Rio de Janeiro, Instituto de Microbiologia Paulo de Góes, RJ, Brazil

**Thais Amorim**

Universidade Federal do Rio de Janeiro, Instituto de Microbiologia Paulo de Góes, RJ, Brazil

**Ana Maria Botelho**

Universidade Federal do Rio de Janeiro, Instituto de Microbiologia Paulo de Góes, RJ, Brazil

**Ana Teresa Vasconcelos**

Laboratório Nacional de Computação Científica

**Luiz Gonzaga Almeida**

Laboratório Nacional de Computação Científica

**Paul Planet**

University of Pennsylvania, Philadelphia, PA 19104, Department of Pediatrics, Perelman College of Medicine

**Russolina Zingali**

Universidade Federal do Rio de Janeiro, Instituto de Bioquímica Médica, RJ

**Agnes Marie Figueiredo**

Universidade Federal do Rio de Janeiro, Instituto de Microbiologia Paulo de Góes, RJ, Brazil

**Bernadete Ferreira-Carvalho** (✉ [bernadete@micro.ufrj.br](mailto:bernadete@micro.ufrj.br))

Instituto de Microbiologia Paulo de Góes, Centro de Ciências da Saúde, Universidade Federal do Rio de Janeiro - Av. Carlos Chagas Filho, 373, Bloco I / I2-017, Cidade Universitária, Ilha do Fundão, Rio de Janeiro, RJ, Brazil

## Research Article

**Keywords:** Streptococcus pyogenes, drug refractory, persisters, efflux pump, antimicrobial resistance, clinical resistance

**Posted Date:** December 28th, 2020

**DOI:** <https://doi.org/10.21203/rs.3.rs-129287/v1>

**License:**  This work is licensed under a Creative Commons Attribution 4.0 International License.

[Read Full License](#)

---

# Abstract

*Streptococcus pyogenes* (group A *Streptococcus*-GAS) is an important pathogen for humans. GAS has been associated with severe and invasive diseases. Despite the fact that these bacteria remain universally susceptible to penicillin, therapeutic failures have been reported in some GAS infections. Many hypotheses have been proposed to explain these antibiotic-unresponsive infections, however none of them has fully elucidated this phenomenon. In this study, antimicrobial persistence emerged when GAS strains were grown at high cell density. Strong efflux activity was detected, and gene expression assays by real-time qRT-PCR showed upregulation of some genes associated with efflux pumps in persistent cells arising in the presence of penicillin. Subsequent phenotypic reversion and whole-genome sequencing indicated that this event was due to non-inherited resistance mechanisms. The tiny persistent colonies showed downregulation of genes associated with protein biosynthesis and cell growth, as demonstrated by gene expression assays. Moreover, proteomic analyses showed that susceptible cells express higher levels of ribosome proteins. The generation of persistent cells due to high bacterial load might be an important mechanism of clinical resistance in GAS invasive infections that has been overlooked. The phenomenon described here might shed some light on the origin of therapeutic failures in *S. pyogenes* infections.

## Introduction

Group A streptococci (GAS) has long been recognized as one of the most important disease-causing bacteria in humans. These bacteria are associated with different types of infections, including pharyngitis, impetigo, scarlet fever, cellulitis, abscesses, and rare cases of pneumonia and meningitis.<sup>1,2</sup> GAS is also involved in severe invasive infections, including toxic shock syndrome, myositis, and necrotizing fasciitis.<sup>1,2</sup> Additionally, these microorganisms are implicated in post infectious sequelae, including acute rheumatic fever, glomerulonephritis, and pediatric autoimmune neuropsychiatric disorders.<sup>1,2</sup>

GAS isolates are typically susceptible to penicillin.<sup>3</sup> However, studies have reported treatment failures in 20–30% of patients receiving  $\beta$ -lactam therapy.<sup>4,5</sup> Many explanations have been proposed to explain clinical failures of penicillin treatment, including a lack of conformity with the 10-day therapeutic regimen, protection of GAS-susceptible isolates by  $\beta$ -lactamase producers in the pharyngeal microbiota, penicillin tolerance, poor antibiotic penetration into the tonsillar tissues, biofilm formation, and bacterial internalization in host cells.<sup>6,7,8</sup> However, the contribution of each of these mechanisms for drug failures remains unclear.<sup>7</sup>

Thulin et al. observed a high bacterial load in tissue biopsy specimens from 17 patients presenting with GAS disseminated infections (necrotizing fasciitis or severe cellulitis) despite intravenous antibiotic therapy for a prolonged time.<sup>8</sup> Those authors concluded that GAS survival inside macrophages could represent a mechanism preventing bacterial eradication.<sup>8</sup> Despite that, some in vitro studies have

demonstrated the effect of a large bacterial inoculum ( $> 10^8$  cells) in the failure of antibiotics to eliminate *E. coli* and mycobacteria.<sup>9–11</sup> However, these studies focused mostly on pharmacodynamics and the dynamics of large population extinction rather than on the mechanisms underpinning this type of resistance.<sup>9–11</sup> We hypothesized that high cell density (HCD) might also induce non-inherited antimicrobial resistance (antibiotic refractory/persistence) in GAS strains. In fact, our findings demonstrated the appearance of antibiotic-refractory GAS cells at HCD, which was coupled with increased activity of intrinsic multidrug-resistant (MDR) efflux pumps. Cumulatively, this study indicated the inhibition of protein biosynthesis and cell growth as possible key mechanisms conferring antibiotic phenotypic resistance (persistence) to GAS cells.

## Methods

### Bacterial isolates

Two hundred-eleven GAS isolates were used to test the effect of HCD on the emergence of bacterial persistence to  $\beta$ -lactam antibiotics. These isolates consisted of a preexisting bacterial collection that was obtained from microbiology laboratories as anonymous samples of infected patients, from different regions of Brazil, and various clinical sites, the majority being from symptomatic oropharyngeal infection. Isolates were identified by routine methods and confirmed by latex agglutination tests (Streptococcal Grouping Kit; Oxoid, Basingstoke, Hampshire, United Kingdom). *Streptococcus pneumoniae* ATCC49619 was used as a control for minimal inhibitory concentration (MIC) and other antimicrobial susceptibility tests. Because all GAS presented the same pattern of antimicrobial refractory at HCD conditions in our model, the GAS strain (37–97), isolated from oropharynx, was selected for most of the studies on antimicrobial persistence.

### MIC

MIC determination was done using the agar dilution method as recommended by the Clinical & Laboratory Standards Institute (CLSI)<sup>12</sup> with concentrations ranging from 0.0025–8  $\mu\text{g/mL}$  penicillin (Wyeth-Whitehall Ltda, Itapevi, SP, Brazil), 0.125–4  $\mu\text{g/mL}$  cephalexin (Sigma), 0.01–4  $\mu\text{g/mL}$  erythromycin (Sigma, St. Louis, Mo, USA), 0.06–4  $\mu\text{g/mL}$  azithromycin (Sigma; from), 0.01–1  $\mu\text{g/mL}$  clindamycin (Sigma), 0.25–16  $\mu\text{g/mL}$  chloramphenicol (Sigma), and 0.12–16  $\mu\text{g/mL}$  tetracycline (Sigma). The MIC for ethidium bromide (EtBr; Sigma) was determined at concentrations of 0.015–4  $\mu\text{g/mL}$ .<sup>13</sup> Two independent experiments were performed.

### Impact of HCD on persistence to $\beta$ -lactams

GAS ( $n = 211$ ) were grown in 100 mL of Todd Hewitt Broth containing 0.5% (w/v) of yeast extract (THB-Y) at 37°C/6 h in order to reach the exponential phase. After centrifugation, the pellet was resuspended at a concentration of approximately  $1-2 \times 10^{10}$  CFU/mL. A 100- $\mu\text{L}$  aliquot ( $1-2 \times 10^9$  CFU/plate), corresponding to  $2-4 \times 10^7$  CFU/cm<sup>2</sup> of a Petri dish surface with an 8.2-cm diameter, was considered an

HCD inoculum. This cell concentration was chosen based on the bacterial load found in tissue biopsies of GAS infections in the studies of Thulin et al.<sup>8</sup> The experiments were also performed at low cell density (LCD) conditions (experimental control). LCD conditions were achieved using bacterial suspension in the exponential phase with concentrations of  $1-2 \times 10^6$  CFU/plate (corresponding to  $2-4 \times 10^4$  CFU/cm<sup>2</sup>), an inoculum size within the range recommended by the CLSI.<sup>12</sup> Both inocula were independently spread onto THB-Y agar (covered or not with a cellophane membrane) containing a 5% defibrinated sheep blood agar base (BAB) supplemented with concentrations varying from 0.0025 µg/mL to 8 µg/mL penicillin or 0.125 to 4 µg/mL cephalexin. The cells grown (37 °C/18 h) on cellophane membrane at HCD, in the highest concentration of antimicrobials, were removed for CFU determination. To test whether defibrinated sheep blood interfered with the analysis, the experiments were also performed in the absence of blood. Three independent experiments were carried out in triplicate.

## Proteomic analysis

A proteomic analysis was done to assess differential protein expression in GAS cells grown at HCD versus LCD. The strain 37-97 was grown at 37 °C for 18 h on cellophane membranes placed on the surface of BAB. Cells were collected, suspended in phosphate buffered saline (PBS) (140 mM NaCl; 2.7 mM KCl; 8 mM Na<sub>2</sub>HPO<sub>4</sub> and KH<sub>2</sub>PO<sub>4</sub> 1.5 mM; pH 7.2), to OD<sub>600nm</sub> = 0.4. Pellet was washed twice, resuspended in PBS and lysed with 106 µm beads (Sigma, USA) in a Bio101 Fast Prep system (BioSavant, Qbiogene, Carlsbad, CA) using six cycles (5 speeds/30 s pulse). After centrifugation, the protein concentration was estimated using a Qubit 2.0 (Invitrogen Life Technologies, CA, USA), and lysates diluted in sodium dodecyl sulfate polyacrylamide Gel (SDS-PAGE) sample buffer (1:1, v/v).<sup>14</sup> Proteins were separated using a 12.5% SDS-PAGE gel electrophoresis, and individual bands were isolated from the gels. All procedures used for the treatment of gel slices and trypsin digestion were performed as previously described.<sup>15</sup> The resulting peptides were desalted using an in-house reverse-phase microcolumn (POROS R2 resin, Applied Biosystems) and dried by vacuum centrifugation.<sup>16</sup> Peptides were solubilized in 20 µL of 0.1% (v/v) formic acid (FA), and 10 µL were injected into a trap column (Opti-Pak C18, Waters, Milford, MA). Liquid chromatography separation was performed using a reverse-phase capillary column (nanoEase C18, 100 mm × 100 µm, Waters) connected to a nano-HPLC system (Waters UPLC, Waters). The eluted peptides were introduced into an ESI-Q-TOF-MS/MS (Q-TOF Micro, Waters) controlled by MassLynx software (Version 4.1, Waters). Mass spectra (MS) were collected in the 50–2.000 m/z range, and the three most abundant ions (charges + 2, +3, and + 4) were submitted for collision-induced dissociation (CID) using argon gas at 13 psi and 18–45 V. The raw data were converted to a peak list using the ProteinLynx Global software (version 4.0, Waters). Protein identification was considered valid if at least one peptide with minimum of 10 amino acids was observed with a maximum error tolerance of 50 ppm and Mascot score  $\geq 46$  ( $p \leq 0.05$ ). The GenBank (Acc) access number, locus tag, and gene and protein names were determined using BLASTp (<http://blast.ncbi.nlm.nih.gov/Blast.cgi>). In addition, Uniprot BLAST analysis ([www.uniprot.org/blast](http://www.uniprot.org/blast)) was performed in order to identify homologs in *S. pyogenes* MGAS10750. Only e-values  $\leq 1.0 \times 10^{-3}$  were considered in the database search.

## Efflux pump activity

Efflux pump activity was tested using a universal pump substrate: ethidium bromide (EtBr).<sup>13</sup> EtBr (0.015–4.0 µg/mL) were incorporated into BAB (covered or not with cellophane membrane), and the strain 37–97 were inoculated at LCD or HCD. The cells grown on cellophane at HCD, in the highest concentration of antimicrobials, were removed for CFU determination. Three individual experiments were performed in triplicate.

## **GAS persistence to antimicrobial drugs**

The ability of GAS to produce cells persistent to different antimicrobials in HCD conditions was tested. Strain 37–97 was streaked at LCD or HCD on BAB (covered or not with a cellophane membrane) with erythromycin (0.01–4 µg/mL), azithromycin (0.06–4 µg/mL), clindamycin (0.01–1 µg/mL), chloramphenicol (0.25–16 µg/mL), or tetracycline (0.12–16 µg/mL). Plates were examined after incubation (37 °C/18 h). The cells grown on cellophane at HCD, in the highest concentration of antimicrobials, were removed for CFU determination. Three independent experiments were performed in triplicate.

## **Effect of cyanide 3-chlorophenylhydrazone (CCCP) efflux pump inhibitor in antimicrobial refractory**

CCCP (Sigma) at 100 µM final concentration<sup>17</sup> was incorporated to BAB (covered or not with a cellophane membrane) supplemented with each antimicrobial drugs or EtBr (at the highest concentrations tested). GAS was spread under LCD or HCD conditions and the plates were incubated at 37°C/18 h. BAB without CCCP were used to control bacterial growth. Three independent experiments were performed in triplicate.

## **Phenotypic switching**

Persistent GAS cells of strain 37–97 grown on BAB containing 8 µg/mL penicillin were subjected to successive passages (up to 500 generations) on BAB without antibiotics. After passaging, bacterial growth was adjusted to 0.5 McFarland, and the penicillin MIC was determined using the agar dilution method (CLSI).<sup>12</sup> Three independent experiments were performed in triplicate.

## **Whole-genome sequencing**

Total DNA from penicillin-persistent and -susceptible cells of the strain 37–97 was obtained using the Wizard Genomic DNA Purification Kit (Promega; Madison, WI, USA). Genomic libraries were prepared using the Nextera XT kit (Illumina, San Diego, CA, USA) and sequenced on an Illumina HiSeq (125 pb reads). The genome assembly was carried out using Newber v3.0.<sup>18</sup> Scaffolds were aligned against a reference genome (*S. pyogenes* strain NGAS743; Acc: CP007560) using cross\_match (version 0.990329; [www.phrap.org/phrap.docs/phrap.htm](http://www.phrap.org/phrap.docs/phrap.htm)). Intra-scaffold and inter-scaffold gaps resulting from repetitive sequences were resolved by in silico gap filling. Any remaining gaps in the genomic sequence from penicillin-persistent cells of the 37–97 strains (37-97P) were filled with "N" with estimated sizes based on the complete sequence of strain 37–97 (37-97S). The sequenced genomes were annotated using RAST 2.0v.<sup>19</sup> Differences in single nucleotide polymorphisms (SNPs) between samples 37-97S and 37-97P

were evaluated using `cross_match` with parameter `discrep_lists`. The generated list was compared to the newbler assembly `ace` file and genome annotation. SNPs were verified by resequencing on an ABI 3730 DNA Analyzer (Life Technologies – Applied Biosystem; Carlsbad, CA, USA). Reactions were performed using the BigDye Terminator v3.1 Cycle Sequencing Kit in 36-cm capillaries with POP7 polymer according to the manufacturer's instructions.

## Gene expression analysis

RNA was prepared from 37–97 cells grown at HCD condition on cellophane membranes plated on 8 µg/mL penicillin BAB. Despite their effect as proton motive force inhibitor, CCCP has also been described as a transcriptional inhibitor of a gene associated with transport<sup>20</sup>. Therefore, for some experiments, gene expression was also performed in presence of CCCP 100 µM. To test the effect of clindamycin in the expression of the efflux-associated locus *MGAS10750\_Spy1819*, total RNA was prepared from 37–97 cells at HCD condition on BAB containing 1 µg/mL (100xMIC) clindamycin. In addition, RNA was also prepared from susceptible cells of 37–97 grown on BAB without antibiotics at LCD conditions. Total RNA was prepared using the RNeasy Mini kit (Qiagen; Maryland, USA) and quantified by a Qubit 2.0 Fluorometer (ThermoFisher Scientific Brasil; São Paulo, Brazil). RNA quality was analyzed by gel electrophoresis. The real-time quantitative reverse transcriptase PCR (real-time RT-qPCR) was performed using Power SYBR Green RNA-to-CT™ 1-Step Kit (Applied Biosystems; Foster City, CA, USA) as recommended ("Guide to Performing Relative Quantitation of Gene Expression Using Real-Time Quantitative PCR"; Applied Biosystems). The rRNA 16S gene was used as an endogenous control. The calibrator sample was total RNA from susceptible cells of strain 37–97. The reaction was performed in a Step One™ Real Time PCR System (Applied Biosystems). Data were analyzed using Step One Software 2.2 (Applied Biosystems). All primers were validated as recommended in the cited guide and listed in Supplementary Table S1. In all tests, at least two independent experiments were performed in triplicate.

## Statistical tests

Two-tailed unpaired Student's t test was used to test the significance of the binary tests for most of the analyses. To analyze the hypothesis that the expression of some efflux pump-associated genes increases in the persistent GAS cells one-tailed unpaired t test was calculated using GraphPad Prism version 9.00 for windows (GraphPad Software, La Jolla, CA, USA). The significance level applied was 0.05. In addition, to confront the null hypothesis, Scaled Jeffreys–Zellner–Siow (JZS) Bayes Factor for two-samples t test was calculated to test the alternative hypothesis for  $r = 0.707$ .<sup>21</sup>

## Results

### Generation of persistence to β-lactam antibiotics

As expected, all GAS tested ( $n = 211$ ) for MIC determinations were susceptible to penicillin, and MIC values varied from 0.0025–0.02 µg/mL. Both MIC50 and MIC90 were 0.01 µg/mL. However, under HCD conditions, all 211 GAS tested grew by forming extremely tiny hemolytic colonies on the surface of BAB

plates containing penicillin concentrations as high as 8 µg/mL (800xMIC) (Fig. 1a, 1b and 1c). However, no GAS growth was detected on 8 µg/mL-penicillin plates containing  $1-2 \times 10^6$  CFU/plate (Fig. 1c). To observe a possible influence of defibrinated sheep blood on persistence generation, GAS strain 37-97 was grown at HCD conditions on BAB plates or on blood agar base without blood supplementation, both containing 8 µg/mL penicillin. Persistent cells were formed in both conditions. Similar to the results obtained for penicillin, persistent cells could also be generated at HCD conditions on BAB plates containing 4 µg/mL (8xMIC) cephalexin (Fig. 1a). The average of persistent cells recovered from 8 µg/mL penicillin-plate was  $1.6 \pm 0.5 \times 10^9$  CFU/mL, corresponding to 2.7% of the total cell population grown at HCD condition without penicillin ( $6.0 \pm 2.4 \times 10^{10}$  CFU/mL). Likewise, the mean value for persistent cells grown on 4 µg/mL-cephalexin plates was  $1.1 \pm 0.1 \times 10^9$  CFU/mL, corresponding to 1.8% of the total cell population grown at HCD condition without penicillin ( $6.0 \pm 2.4 \times 10^{10}$  CFU/mL) (Fig. 1b).

Despite the persistence observed, drug susceptibility could be reverted when cells were submitted to serial passaging on BAB plates without antibiotics, with previously persistent cells returning to their original state of drug susceptibility (MIC = 0.01 µg/mL). Additionally, DNA from penicillin-persistent and susceptible cells of strain 37-97 underwent whole-genome sequencing (WGS). Both sequences were identified as *S. pyogenes* ST62. WGS alignments generated in MAUVE showed high identity and perfect synteny of collinear blocks (Fig. 2a). There was also no difference in the absence or presence of mobile genetic elements, genomic islands, or unique genes in the persistent cells (Acc: CP041615) compared with that of susceptible ones (Acc: CP041408). Despite some differences in SNPs observed in the WGS, these could not be confirmed by Sanger resequencing of these regions, thus mutations were not associated with the emergence of persistent cells (Fig. 2b).

### Proteomic analysis

A total of 79 proteins were only detected when GAS strain 37-97 was grown in LCD conditions (Supplementary Table S2 online), 61 were only detected at HCD (Supplementary Table S3 online), and 128 were found in both density conditions (Supplementary Table S4 online). The most remarkable feature was the low frequency of L ribosomal proteins (LRP) in GAS cells grown at HCD (3.3%). However, the most frequently detected proteins under LCD conditions were the LRP proteins (31.6%), which play essential roles in ribosome assembly and are crucial for protein synthesis and cell growth (Fig. 3). These data suggest a decrease in growth activity under HCD conditions, which is consistent with the tiny colonies formed by persistent cells. Some multidrug resistance (MDR) efflux pump components were only detected under HCD conditions, including a protein associated with the periplasmic component of the efflux system that belongs to the root-nodulation-cell-division (RND) family (Uniprot access: Q1J790). Multiple sugar transport ATP-binding protein MsmK (Uniprot access: Q1J4L0) and the multidrug resistant ABC transporter ATP-binding and permease protein (Uniprot access: Q1J8L9) were also observed under HCD conditions (Supplementary Table S3 online).

### Efflux pump activity

A universal efflux pump substrate, EtBr, was used to compare the efflux pump activity between cells grown at HCD and LCD conditions. The MIC value of strain 37–97 for EtBr was 0.06 µg/mL. However, when bacteria were grown at HCD conditions, growth was observed at concentrations of EtBr as high as 4 µg/mL (Fig. 4a), indicating intense efflux activity under conditions that generate persistent GAS cells. The number of EtBr-refractory cells recovered at concentration of 4 µg/mL were  $3.3 \pm 0.9 \times 10^9$  CFU/mL, corresponding to 6% of the GAS cell population grown in BAB plates in the absence of EtBr at HCD condition without EtBr ( $5.5 \pm 2.0 \times 10^{10}$  CFU/mL) (Fig. 4b).

Because antibiotics are well-known substrates of efflux pumps, to further analyze the role of these pumps in antibiotic persistence, we also tested other types of antimicrobials under HCD conditions. The data showed that under HCD conditions, antibiotic persistence arose for all antimicrobials tested independent on the class of the drug analyzed. Persistent cells grew at MIC levels and concentrations as high as 4 µg/mL (33xMIC) erythromycin, 4 µg/mL (33xMIC) azithromycin, 1 µg/mL (100xMIC) clindamycin, 16 (16xMIC) µg/mL chloramphenicol, and 16 µg/mL (133xMIC) tetracycline (Fig. 4a). The percentage of persistent cells recovered, considering all antimicrobials tested, ranged from  $1.7 \pm 0.1 \times 10^8$  CFU/mL (0.32%) to  $2.7 \pm 1.7 \times 10^9$  CFU/mL (5.0%). In relation to the cell population ( $5.5 \pm 2.0 \times 10^{10}$  CFU/mL) grown at HCD condition without antimicrobials (Fig. 4b).

Since the resistance-nodulation-division (RND) family of efflux pumps was one of the drug/proton antiporters detected in the proteome under HCD conditions, we used the pump inhibitor CCCP to dissipate the proton-motive force. Control plates with CCCP (100 µM) without antibiotic cause no effect on bacterial growth. Despite the inhibition by CCCP of persistent cells to clindamycin and chloramphenicol (Fig. 4c), this compound did not inhibit persistence to β-lactams or other antimicrobials tested.

### Gene expression analysis

Of the 15 genes analyzed that were associated with the efflux pumps, seven showed some levels of upregulation in penicillin-persistent cells compared with those of susceptible GAS cells (Fig. 5a). Among these, genes of an operon associated with efflux pumps of the RND family showed increases of  $\geq 4$ -fold, which included *MGAS10750\_Spy1817* (gene product: ABC transporter ATP binding protein;  $p = 0.0156$ ), *MGAS10750\_Spy1818* (gene product: ABC transporter permease protein;  $p = 0.0088$ ), and *MGAS10750\_Spy1819* (gene product: periplasmic component of efflux system,  $p < 0.0001$ ). An increase in transcripts of  $> 4$ -fold was also observed for a gene product annotated as belonging to a major facilitator superfamily, the multidrug resistance protein B (*MGAS10750\_Spy0495*) ( $p = 0.04$ ). Another gene upregulated was a homolog of the multiple sugar transport ATP-binding protein *msmK* (*MGAS10750\_Spy1776*), which displayed a 2.2-fold increase in expression levels, however this value was not statistically significant ( $p = 0.1490$ ). The loci *MGAS10750\_Spy0043* and *MGAS10750\_Spy1633* (*norA* homologue) showed about 2-fold increase ( $p < 0.0001$  and  $p = 0.0031$ , respectively; Fig. 5a).

Because clindamycin was one of the antibiotics completely inhibited by CCCP, we also investigated the effect of antibiotic in the overexpression of *MGAS10750\_Spy1819*, which is part of the ABC transport

operon. Our data showed an increase of about 9-fold in the expression of this gene. It was observed that CCCP had simultaneously affected the transcript levels of this ABC operon and two genes homologs to *ihk* (*MGAS10750\_Spy1815*) and *irr* (*MGAS10750\_Spy1816*) encoding the two-component regulatory system (TCS) Ihk/Irr, which are adjacent to and upstream this operon. Our data showed that both the operon and two-component regulator were downregulated in the presence of CCCP (ABC operon:  $p = 0.03$ ,  $p = 0.021$ ,  $p = 0.0009$  and *ihk/irr*:  $p = 0.0057$ ,  $p = 0.0389$ , respectively; Fig. 5b). Similar to the downstream genes belonging to the ABC operon, *ihk/irr* homologs also displayed increased levels of transcripts (4-fold) for persistent cells grown in the absence of CCCP ( $p = 0.0006$  and  $p = 0.01$ ), compared with the susceptible GAS cells grown at LCD (Fig. 5b). These data suggest that the *Ihk/Irr* system could be acting as a regulator of this operon. Indeed, consistent with an increase in pump activity, genes (*MGAS10750\_Spy1765* and *MGAS10750\_Spy1120*) annotated as belonging to the MarR and GntR families (pump negative transcriptional regulators) were significantly downregulated in the persistent cells ( $p = 0.0032$  and  $p = 0.0137$ ; Fig. 5c).

Additionally, the expression of genes associated with protein biosynthesis and cell growth/division were evaluated. For all these genes, the transcript levels decreased, but for *bcaT* homolog (gene product: branched-chain-amino acid aminotransferase) this decrease was not significant. The *guaA* homolog (gene product: GMP synthesis [glutamine hydrolyzing]), which is involved in the GTP pathway, was 2-fold down-regulated ( $p = 0.016$ ). Decreased expression was also observed for *relA* (gene product: GTP pyrophosphokinase;  $p = 0.003$ ) and *typA* (gene product: GTP-binding protein TypA/BipA;  $p = 0.0314$ ). Finally, the *ftsA* homolog, which is essential for cell division, was reduced 3-fold ( $p = 0.0187$ ) (Fig. 5d).

Among the genes associated with the stress conditions studied, which includes some genes related to oxidative stress, the majority was down-regulated in penicillin-persistent GAS cells. A significant increase was only observed for a *dpr* homolog (gene product: hydrogen peroxide resistance regulator), which was about 2-fold ( $p = 0.03$ ) more expressed compared with the susceptible GAS cells (Fig. 5e). Finally, we examined the expression of three genes homologous to toxin-antitoxin (TA) systems found in the genome of *S. pyogenes* strain 37-97. Increased expression was only observed for the *hicA/B* homologs (2.8-fold and 3.5-fold increase, respectively;  $p = 0.007$  and  $p = 0.017$ , respectively) for persistent cells (Fig. 5f).

## Discussion

The influence of the bacterial inoculum on antimicrobial resistance in vitro has been described by others.<sup>22-24</sup> Despite the fact that it might be a reason for antimicrobial failures in antibiotic treatment, the mechanisms involved in this type of resistance remain mostly unexplored. To the best of our knowledge, this phenomenon has not been reported for GAS strains, thus far. Here, we showed that a relatively large number of GAS cells (calculated as  $10^7$ - $10^8$  CFU/plate) became persistent to various classes of antimicrobials under HCD conditions, corresponding to about 0.3 to 6% of the total bacterial population. It is important to emphasize that drug persistence was not a particular characteristic of only one or a few representatives of GAS because all 211 isolates from our collection demonstrated the same phenomenon. Furthermore, this resistance could not be attributed to the Eagle effect,<sup>25</sup> since persistent

GAS cells were also recovered not only at high antibiotic concentrations but also at MIC levels for all antimicrobials tested at the HCD condition. Phenotypic reversion was observed, indicating the involvement of non-inherited antimicrobial resistance mechanisms. There is no question that bacterial resistance acquired through genetic mechanisms is the major reason for clinical failures during antimicrobial therapy for many other pathogens. However, the importance of non-inherited resistance should not be disregarded, mainly concerning infections affecting immunocompromised patients, those associated with biofilm production, or severe and invasive infections where a high bacterial load can accumulate at the site of infection.<sup>8</sup>

It was observed that CCCP fully restored the susceptibility to clindamycin and chloramphenicol, suggesting the involvement of proton efflux pumps in GAS persistence/refractory to these drugs. In fact, a gene of the ABC operon of the RND family (that uses proton gradient force across inner membrane to exclude drugs)<sup>26</sup> was almost 9-fold overexpressed in GAS-persistent cells induced by clindamycin. It is possible that additional efflux pumps, not importantly affected by CCCP, may be involved in the extrusion of the other antimicrobials tested. This assumption is supported by the fact that CCCP did not recover GAS susceptibility to the universal pump substrate EtBr at HCP condition. Indeed, about 50% of the efflux-associated genes analyzed were upregulated in penicillin-resistant cells generated under HCD conditions.

Typically, overexpression of efflux pumps confers resistance to different classes of antimicrobial agents and some dyes, such as EtBr, in other bacterial species.<sup>27-30</sup> The involvement of conserved RND proteins in reducing *S. aureus* persistence to  $\beta$ -lactams and glycopeptides has also been demonstrated.<sup>31</sup> Poudyal and Sauer found increased expression of genes associated with an ABC transporter and other transport systems in *Pseudomonas aeruginosa* grown in biofilms, suggesting these mechanisms contributed to the persistence phenotype of *P. aeruginosa* to tobramycin.<sup>32</sup> Indeed, in our study, a homolog of *marR*, a negative pump regulator, was down-regulated in persistent cells. In line with these data, increased resistance in *Burkholderia thailandensis* was attributed to enhanced efflux pump activity and was detected after repression of a *marR* homolog.<sup>33</sup> Additionally, we found that a gene in the GntR family of regulators was also down-regulated in penicillin-persistent GAS cells. It is remarkable that a *norG* knockout in *S. aureus* (a member of the GntR family) led to a 3-fold increase in the expression of an *abcA* gene encoding a protein of the ABC transport system with a concomitant increase in resistance to  $\beta$ -lactams.<sup>34</sup>

The Ihk/Irr two-component system is involved in the regulation of various streptococcal processes, including virulence.<sup>35,36</sup> It is notable that *ihk/irr* were overexpressed in a non-human primate model of GAS necrotizing myositis, and these genes were implicated in GAS resistance to polymorphonuclear phagocytosis.<sup>36</sup> The fact that CCCP inhibited *ihk/irr* gene regulators and the RND family operon concomitantly, and that both the operon and regulators displayed increased expression in GAS-persistent cells, raises an interesting hypothesis about another possible role for the Ihk/Irr system besides virulence regulation. However, despite the gene co-localization and the concomitant regulation of *ihk/irr* and the

genes of the ABC transport operon by CCCP, molecular cloning strategies are needed to validate the hypothesis that *ihk/irr* may not only regulate GAS virulence but also this transport system.

Oxidative stress has also been associated with antimicrobial persistence in *E. coli*.<sup>37</sup> In that study, a *dpr* homolog was upregulated in penicillin-resistant GAS cells. The *dpr* gene encodes the non-specific DNA binding protein Dps (peroxide resistance protein, Dpr), and homologs have been identified in different bacterial species associated with protection against multiple stressors.<sup>38</sup> Dps protein forms self-aggregates and an insoluble complex with DNA. In *E. coli*, the aggregates formed in the stationary growth phase correlated with increased persistence.<sup>38</sup> Also, the induction of *dps* in *E. coli* resulted in overexpression of the toxin/antitoxin (TA) system MqsR/MqaA<sup>39</sup>. In fact, in our study, the TA system of the HicAB family was upregulated in GAS-persistent cells. However, the role of the TA system in *E. coli* persistence remains controversial.<sup>40</sup>

In addition to efflux pumps, stress conditions, and TA systems, slow-growing cells and stringent responses have also been implicated in antimicrobial persistence.<sup>40</sup> The persistent GAS cells produced tiny colonies, suggesting a condition of slow growth. In fact, genes associated with protein biosynthesis were down-regulated in the penicillin-persistent GAS cells, including homologs of *typA/bipA* (important in ribosome assembly) and *guaA* (essential in GTP synthesis). These results agree with the proteomic data that showed increased expression of ribosome protein L in GAS cells grown at LCD in comparison with the expression observed at HCD. Indeed, the expression of the *ftsA* gene, which is essential for cell growth, was reduced in penicillin-persistent GAS cells. It is notable that a substantial reduction in transcription and translation was previously observed for antimicrobial-persistent *E. coli*, which was associated with increased expression of different RNases (including RNase E, which is involved in the specific degradation of *ftsA-ftsZ* transcripts).<sup>41</sup>

In conclusion, we showed that GAS cells grown at HCD condition can become persistent to high concentrations of  $\beta$ -lactams and other antimicrobials. Our data indicate that increased efflux pump activity and slow cell growth are mechanisms associated with this phenotypic resistance in GAS cells, which has been observed for other persistent bacteria. It is possible that this phenomenon might have some implications for failures in antimicrobial therapy that have been reported for some GAS clinical infections,<sup>4,5</sup> including those severe and sometimes lethal invasive diseases, for which high bacterial load can be achieved in the infected tissues, despite the use of (in vitro) effective antimicrobial therapy<sup>8</sup> and thus it should not be overlooked. Finally, it is likely that studies with *ihk/irr* could elucidate a role of the upregulation of these genes not only in the increase of intracellular persistence of GAS in macrophages, but also in the emergence of antimicrobial persistence.

## Declarations

## Acknowledgements

The authors thank Mrs. Raquel Neves for her excellent technical assistance. We are very grateful Dr. Clemente Aguilar for his assistance with the Blast2Go software, and to Ms. Ana L. Carvalho for her help with the LC-MS/MS analysis.

### Author contributions

Conception and design of the work: AMSF, BTFC and RBZ. The experiments were carried out by AZC, CLM, CNG, MCM, MCNM, TTA and USL. Data were analyzed and interpreted by AMSF, AZC, BTFC, CLM, and RBZ. The whole genome sequencing and analysis were performed by AMNB, ATRV, LGPA and PJP. The manuscript was written and revised by AMSF, BTFC and CLM. All authors approved the final version of the manuscript.

### Competing interests

The authors declare no competing interests.

### Funding

CLM was awarded with PhD fellowships from Coordenação de Aperfeiçoamento de Pessoal de Nível Superior (CAPES) – Brasil, Finance Code 001 and Conselho Nacional de Desenvolvimento Científico e Tecnológico (CNPq). AZC was awarded with PhD fellowship from Conselho Nacional de Desenvolvimento Científico e Tecnológico (CNPq).

### Data availability

All data will be made openly available upon publication of this manuscript.

## References

1. Ralph, A.P. & Carapetis, J.R. Group A streptococcal diseases and their global burden. *Curr. Top. Microbiol. Immunol.* 368, 1–27 (2012).
2. Gerardi, D.M., Casadonte, J., Patel, P. & Murphy, T.K. PANDAS and comorbid Kleine–Levin Syndrome. *J Child Adolesc Psychopharmacol.* 25, 93–98 (2015).
3. Zacharioudaki, M.E. & Galanakis, E. Management of children with persistent group A streptococcal carriage. *Expert Rev Anti Infect Ther.* 15, 787–795 (2017).
4. Gidengil, C.A., Kruskal, B.A. & Lee, G.M. Initial antibiotic choice in the treatment of group A streptococcal pharyngitis and return visit rates. *J Pediatric Infect Dis Soc.* 2, 361–367 (2013).
5. Brook I. Overcoming penicillin failures in the treatment of Group A streptococcal pharyngo-tonsillitis. *Int J Pediatr Otorhinolaryngol.* 71, 1501–1508 (2007).
6. Fiedler, T., Köller, T. & Kreikemeyer, B. *Streptococcus pyogenes* biofilms formation, biology, and clinical relevance. *Front Cell Infect Microbiol.* 5, 1–11 (2015).

7. Walker, M.J. *et al.* Disease manifestations and pathogenic mechanisms of group A *Streptococcus*. *Clin Microbiol Rev.* 27, 264–301 (2014).
8. Thulin, P. *et al.* Viable group A Streptococci in macrophages during acute soft tissue infection. *PLoS Med.* 3, e53; 10.1371/journal.pmed.0030053 (2006).
9. Nielsen, E.I., Cars, O. & Friberg, L.E. Predicting in vitro antibacterial efficacy across experimental designs with a semimechanistic pharmacokinetic-pharmacodynamic model. *Antimicrob Agents Chemother.* 55, 1571–1579 (2011).
10. Ferro, B.E., van Ingen, J., Wattenberg, M., van Soolingen, D. & Mouton, J.W. Time-kill kinetics of antibiotics active against rapidly growing mycobacteria. *J Antimicrob Chemother.* 70, 811–817 (2015).
11. Coates, J. *et al.* Antibiotic-induced population fluctuations and stochastic clearance of bacteria. *Elife.* 7, 1–26 (2018).
12. Cockerill, F.R. *et al.* Performance Standards for Antimicrobial Susceptibility Testing: Twenty-First Informational Supplement. *Clinical and Laboratory Standards Institute.* 31 (2011).
13. Hsieh, P.C, Siegel, S.A., Rogers, B., Davis, D. & Lewis, K. Bacteria lacking a multidrug pump: A sensitive tool for drug discovery. *Proc Natl Acad Sci.* 95, 6602–6606 (1998).
14. Laemmli U. Cleavage of structural proteins during the assembly of the head of bacteriophage T4. *Nature.* 227, 680–685 (1970).
15. Shevchenko, A., Wilm, M., Vorm, O. & Mann, M. Mass spectrometric sequencing of proteins from silver-stained polyacrylamide gels. *Anal Chem.* 68, 850–858 (1996).
16. Rodrigues, S.P. *et al.* Proteomic analysis of papaya (*Carica papaya* L.) displaying typical sticky disease symptoms. *Proteomics.* 11, 2592–2602 (2011).
17. Clancy, J. *et al.* Molecular cloning and functional analysis of a novel macrolide-resistance determinant, *mefA*, from *Streptococcus pyogenes*. *Mol Microbiol.* 22, 867-879 (1996).
18. Margulies, M. *et al.* Genome sequencing in microfabricated high-density picolitre reactors. *Nature.* 437, 376–380 (2005).
19. Overbeek R. *et al.* The SEED and the rapid annotation of microbial genomes using subsystems technology (RAST). *Nucleic Acids Res.* 42, D206–D214 (2014).
20. Baron, S.A. & Rolain, J-M. Efflux pump inhibitor CCCP to rescue colistin susceptibility in *mcr-1* plasmid-mediated colistin-resistant strains and Gram-negative bacteria. *J Antimicrob Chemother.* 73, 1862–1871 (2018).
21. Rouder, J.N., Speckman P.L., Sun D., Morey R.D. & Iverson G. Bayesian t-tests for accepting and rejecting the null hypothesis. *Psychon Bull Rev* 16, 225-237 (2009).
22. Rio-Marques, L., Hartke, A. & Bizzini, A. The effect of inoculum size on selection of in vitro resistance to vancomycin, daptomycin, and linezolid in methicillin-resistant *Staphylococcus aureus*. *Microb Drug Resist.* 20, 539–543 (2014).

23. Karlake, J., Maltas, J., Brumm, P. & Wood, K.B. Population density modulates drug inhibition and gives rise to potential bistability of treatment outcomes for bacterial infections. *PLoS Comput Biol.* 12, e1005098; [10.1371/journal.pcbi.1005098](https://doi.org/10.1371/journal.pcbi.1005098) (2016).
24. Li, J. *et al.* Antimicrobial activity and resistance: influencing factors. *Front Pharmacol.* 8, 364; [10.3389/fphar.2017.00364](https://doi.org/10.3389/fphar.2017.00364) (2017).
25. Harry, E. & Musselman, A.D. The rate of bactericidal action of penicillin in vitro as a function of its concentration, and its paradoxically reduced activity at high concentrations against certain organisms. *J Exp Med.* 88, 99–131 (1948).
26. Eicher, T. *et al.* Coupling of remote alternating-access transport mechanisms for protons and substrates in the multidrug efflux pump AcrB. *eLife*, 3; [10.7554/eLife.03145](https://doi.org/10.7554/eLife.03145) (2014).
27. Sun, J., Deng, Z. & Yan, A. Bacterial multidrug efflux pumps: Mechanisms, physiology and pharmacological exploitations. *Biochem Biophys Res Commun.* 453, 254–267 (2014).
28. Martins, M. *et al.* Identification of efflux pump-mediated multidrug-resistant bacteria by the ethidium bromide-agar cartwheel method. *In Vivo.* 25, 171–178 (2011).
29. Wang, Y. *et al.* LuxS/AI-2 system is involved in fluoroquinolones susceptibility in *Streptococcus suis* through overexpression of efflux pump SatAB. *Vet Microbiol.* 233, 154–158 (2019).
30. DeMarco, C.E. *et al.* Efflux-related resistance to norfloxacin, dyes, and biocides in bloodstream isolates of *Staphylococcus aureus*. *Antimicrob Agents Chemother.* 51, 3235–3239 (2007).
31. Quiblier, C, Zinkernagel, A.S., Schuepbach, R.A., Berger-Bächi, B. & Senn, M.M. Contribution of SecDF to *Staphylococcus aureus* resistance and expression of virulence factors. *BMC Microbiol.* 11, 72; [10.1186/1471-2180-11-72](https://doi.org/10.1186/1471-2180-11-72) (2011).
32. Poudyal, B. & Sauer, K. The ABC of biofilm drug tolerance: the MerR-like regulator BrlR is an activator of ABC transport systems, with PA1874-77 contributing to the tolerance of *Pseudomonas aeruginosa* biofilms to tobramycin. *Antimicrob Agents Chemother.* 62, e01981-17; [10.1128/AAC.01981-17](https://doi.org/10.1128/AAC.01981-17) (2017).
33. Sabrin, A., Gioe, B.W., Gupta, A. & Grove, A. An EmrB multidrug efflux pump in *Burkholderia thailandensis* with unexpected roles in antibiotic resistance. *J Biol Chem.* 294, 1891–1903 (2019).
34. Truong-Bolduc, Q.C. & Hooper, D.C. The transcriptional regulators NorG and MgrA modulate resistance to both quinolones and -lactams in *Staphylococcus aureus*. *J Bacteriol.* 189, 2996–3005 (2007).
35. Han, H. *et al.* The two-component system lhk/Irr contributes to the virulence of *Streptococcus suis* serotype 2 strain 05ZYH33 through alteration of the bacterial cell metabolism. *Microbiology.* 158, 1852–1866 (2012).
36. Kachroo, P. *et al.* New pathogenesis mechanisms and translational leads identified by multidimensional analysis of necrotizing myositis in primates Priyanka. *mBio.* 11; e03363-19; [10.1128/mBio.03363-19](https://doi.org/10.1128/mBio.03363-19) (2020).
37. Wu, Y., Vulić, M., Keren, I. & Lewis, K. Role of oxidative stress in persister tolerance. *Antimicrob Agents Chemother.* 56, 4922–4926 (2012).

38. Leszczynska, D., Matuszewska, E., Kuczynska-Wisnik, D., Furmanek-Blaszczak, B. & Laskowska, E. The formation of persister cells in stationary-phase cultures of *Escherichia coli* is associated with the aggregation of endogenous proteins. *PLoS One*. 8, e54737; 10.1371/journal.pone.0054737 (2013).
39. Kim, Y., *et al.* *Escherichia coli* toxin/antitoxin pair MqsR/MqsA regulate toxin CspD. *Environ Microbiol*. 12, 1105–1121 (2010).
40. Goormaghtigh, F. *et al.* Reassessing the role of type II toxin-antitoxin systems in formation of *Escherichia coli* type II persister cells. *mBio*. 9; 10.1128/mBio.00640-18 (2018).
41. Radzikowski, J.L. *et al.* Bacterial persistence is an active  $\sigma$  S stress response to metabolic flux limitation. *Mol Syst Biol*. 12, 882; 10.15252/msb.20166998 (2016).

## Figures

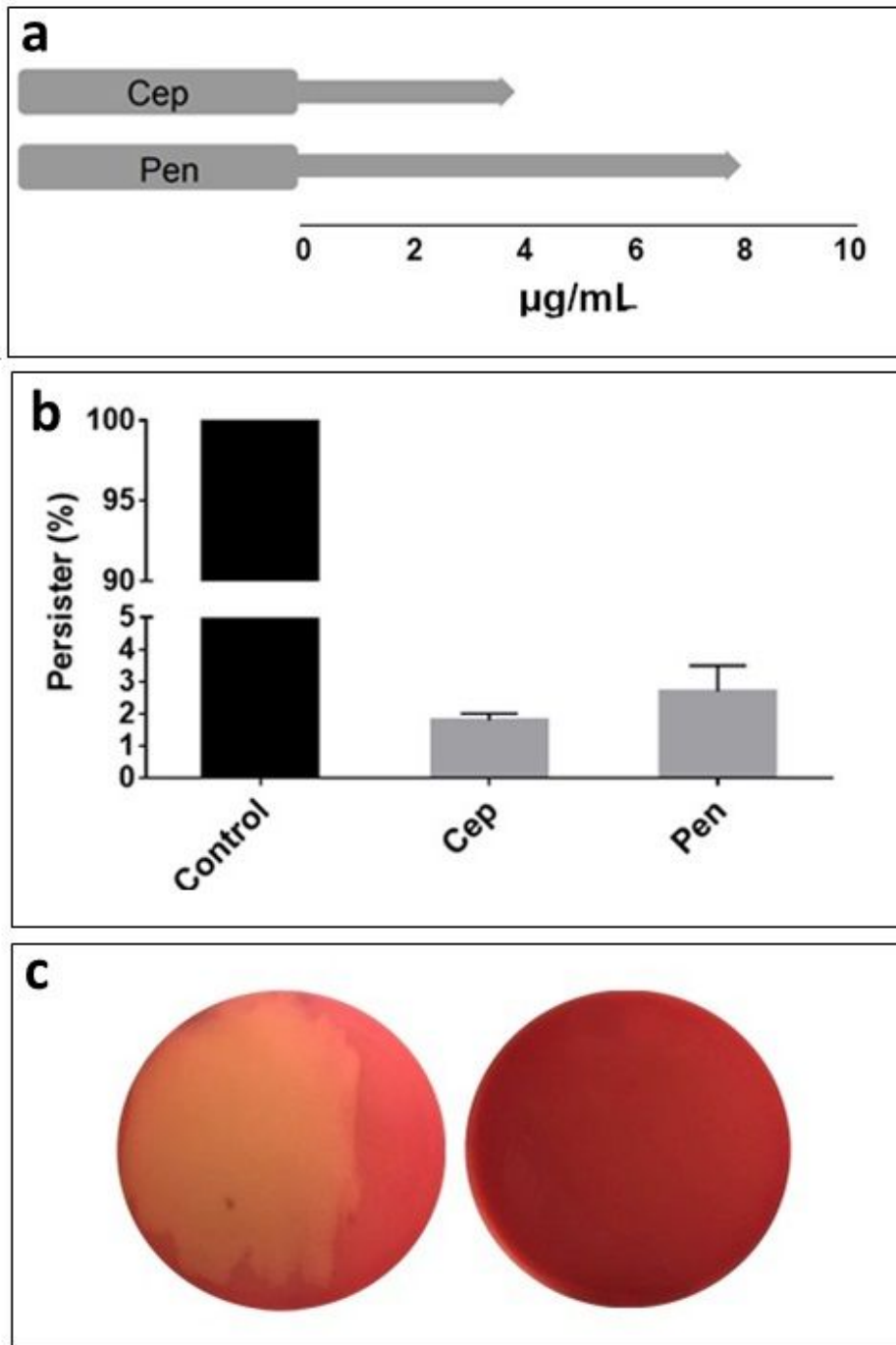


**Figure 1**

Generation of GAS persistent cells in the presence of penicillin and cephalixin. (a) Persistent cells of the strain 37-97 grown at high cell density in the presence of different concentrations of antimicrobials. The arrow indicates the range of drug concentrations in which persistent cells were detected. The tip of arrow indicates the highest concentration used in these experiments. Susceptible cells grown at low cell density showed a MIC of  $0.01 \mu\text{g/mL}$  and  $0.5 \mu\text{g/mL}$  in the presence of penicillin (Pen) and cephalixin (Cep),

respectively. (b) Persistent cells recovered [Persister (%)] from BAS plates containing 8  $\mu\text{g}/\text{mL}$  or 4  $\mu\text{g}/\text{mL}$  of penicillin and cephalexin, respectively. (c) Left plate: Generation of tiny and hemolytic colonies of persistent cells on blood agar base plates containing 8  $\mu\text{g}/\text{mL}$  penicillin inoculated with the GAS strain 37-97 at high cell density. Right plate: Absence of growth on blood agar base plates containing 8  $\mu\text{g}/\text{mL}$  penicillin inoculated with strain 37-97 at low cell density.

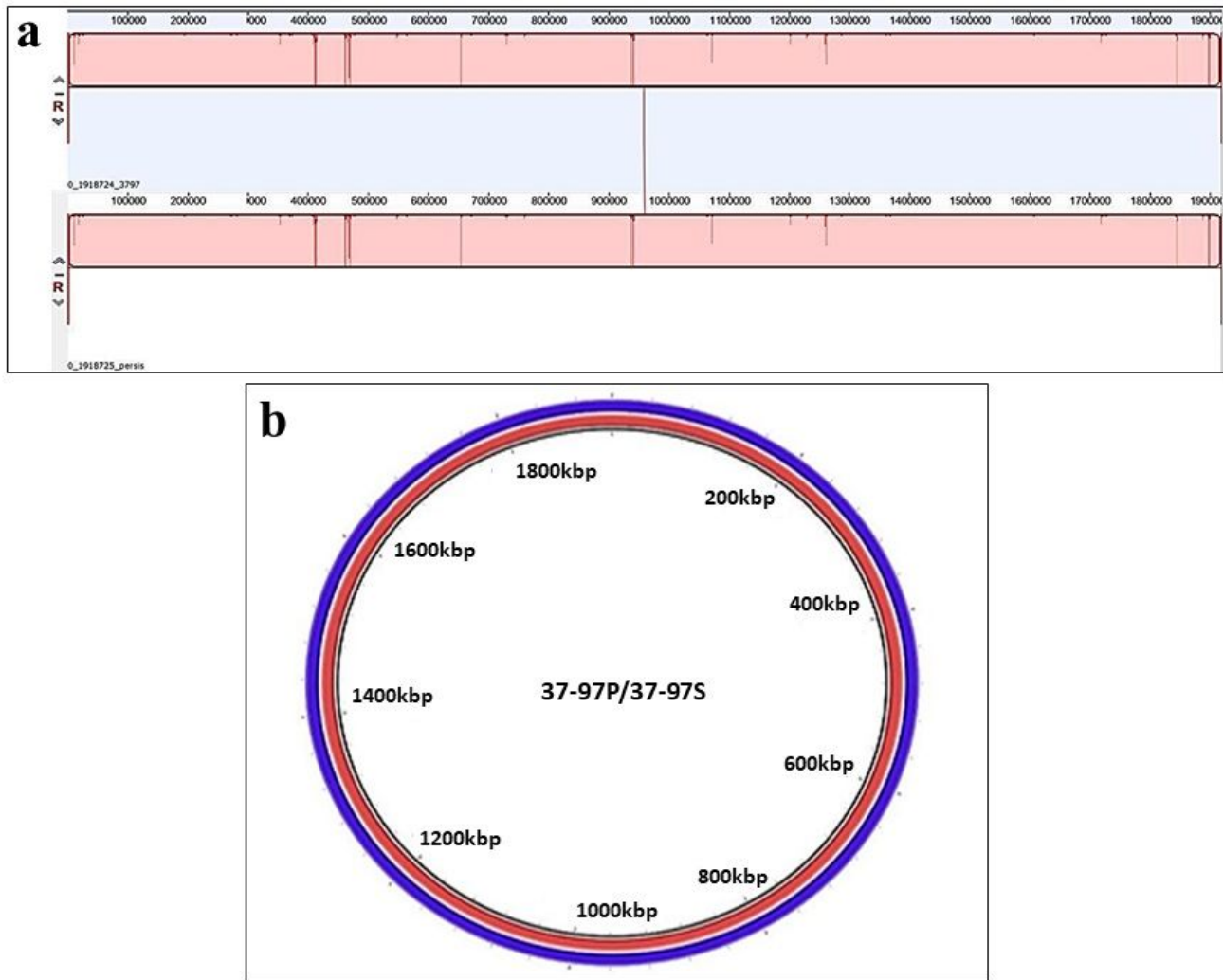


**Figure 2**

Analysis of synteny and circular comparison of the chromosomes. (a) Genome alignments were performed using MAUVE. DNA sequences from persistent cells of strain 37-97 grown on penicillin plates at concentration of 800 X MIC (37-97P) and from susceptible cells of strain 37-97 (37-97S). (b). Circular comparison of the chromosomes was generated by Blast Ring Image Generator (BRIG) using genome sequences obtained from 37-97P (red) and 37-97S (blue). No difference was observed between the two sequences.

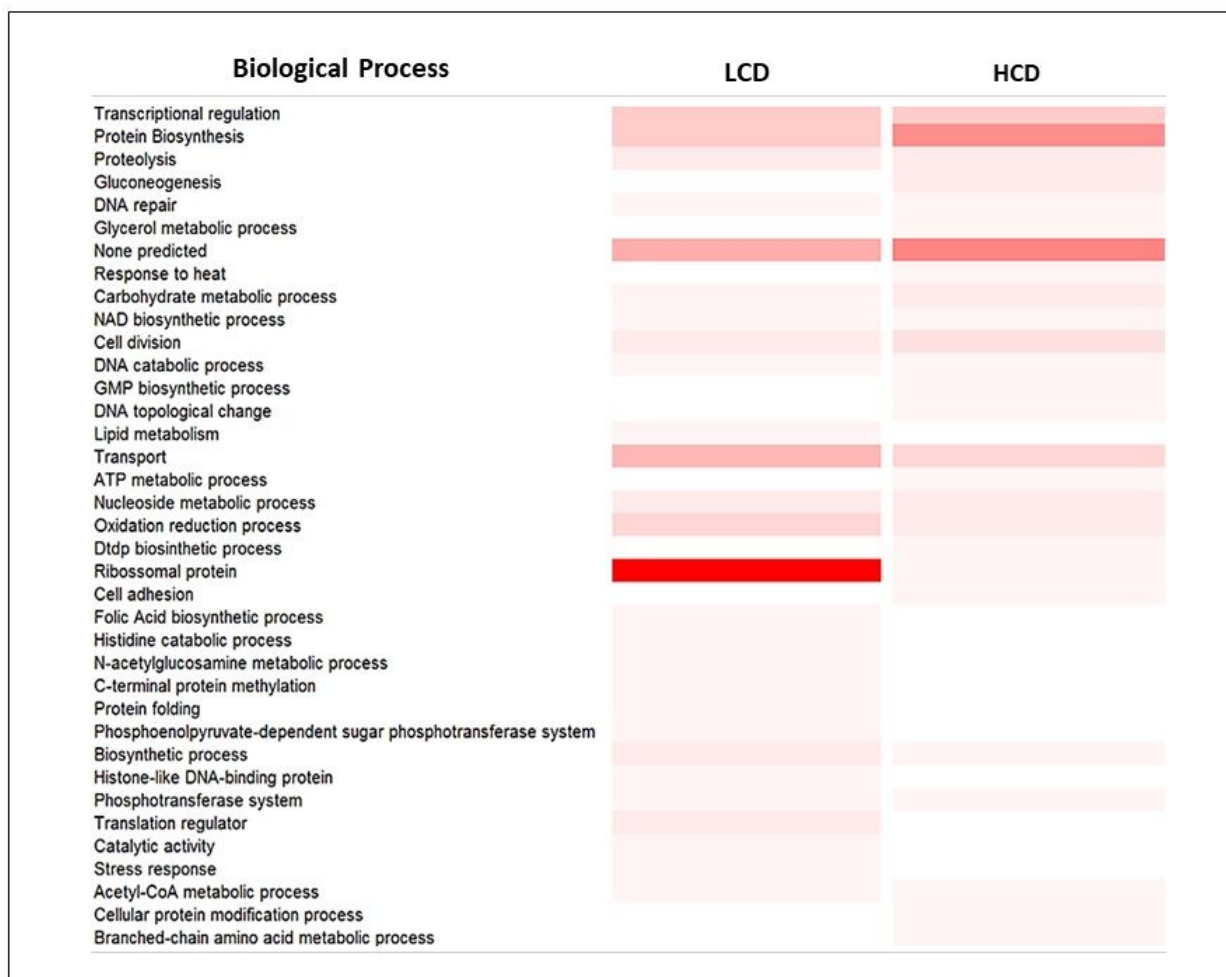


**Figure 3**

Proteomic analysis of GAS strain 37-97 grown at low cell density (LCD) and high cell density (HCD). Color gradient indicates the frequency of proteins involved in a biological process according to InterPro ([www.ebi.ac.uk/interpro](http://www.ebi.ac.uk/interpro)). More intense color: Highest number of proteins. Lightest color: Smallest number of proteins. White color: Absence of proteins.

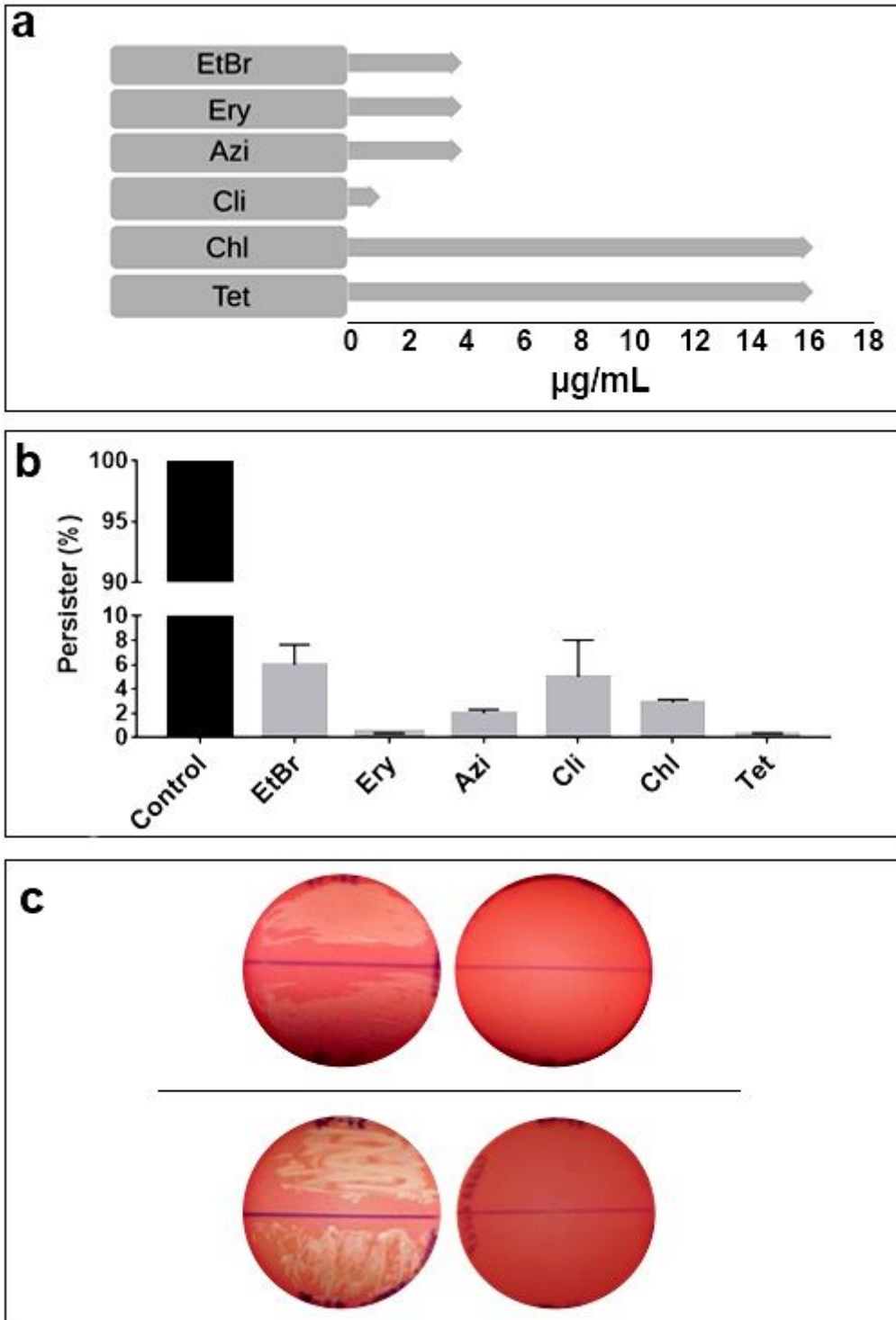


**Figure 4**

Generation of GAS persistent cells in the presence of ethidium bromide and non-β-lactam antimicrobials. (a) Persistent cells of the strain 37-97 grown at high cell density condition in different drug concentrations. The arrow indicates the range of drug concentrations in which persistent cells were detected. The tip of arrow indicates the highest concentration used in these experiments. The drugs tested were ethidium bromide (EtBr), erythromycin (Ery), azithromycin (Azi), clindamycin (Cli), chloramphenicol (Chl) and tetracycline (Tet). Susceptible cells grown at low cell density showed MICs of

0.06  $\mu\text{g}/\text{mL}$  (EtBr), 0.12  $\mu\text{g}/\text{mL}$  (Ery), 0.12  $\mu\text{g}/\text{mL}$  (Azi), 0.01  $\mu\text{g}/\text{mL}$  (Cli), 1  $\mu\text{g}/\text{mL}$  (Chl), or 0.12  $\mu\text{g}/\text{mL}$  (Tet). (b) Percentage of persistent GAS cells [Persister (%)] recovered from BAS plates containing 4  $\mu\text{g}/\text{mL}$  EtBr, 4  $\mu\text{g}/\text{mL}$  Ery, 4  $\mu\text{g}/\text{mL}$  Azi, 1  $\mu\text{g}/\text{mL}$  Cli, 16  $\mu\text{g}/\text{mL}$  Chl, or 16  $\mu\text{g}/\text{mL}$  Tet. (c) Inhibition of antimicrobial persistence by a specific efflux pump inhibitor, cyanide 3-chlorophenylhydrazone (CCCP). Top panel: Left plate was supplemented with 1  $\mu\text{g}/\text{mL}$  clindamycin, and right plate with 1  $\mu\text{g}/\text{mL}$  clindamycin and 100  $\mu\text{M}/\text{mL}$  CCCP. Bottom panel: Left plate was supplemented with 16  $\mu\text{g}/\text{mL}$  chloramphenicol, and right plate with 16  $\mu\text{g}/\text{mL}$  chloramphenicol and 100  $\mu\text{M}/\text{mL}$  CCCP. High population density GAS was inoculated on all plates. Persistence to these antibiotics was completely inhibited in the presence of CCCP.

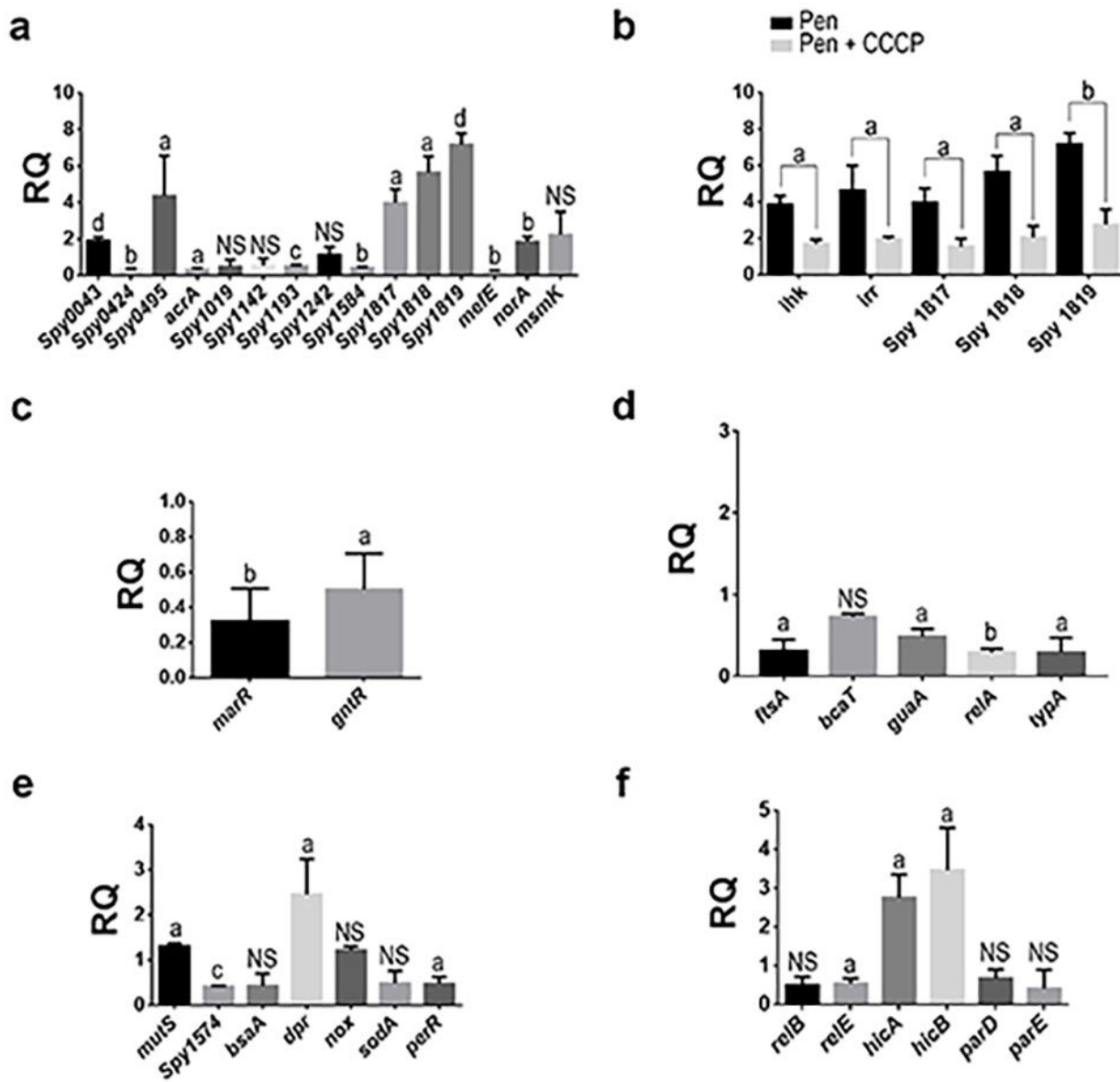


Figure 5

Analysis of the gene expression in penicillin-persistent GAS cells, strain 37-97. (a) Transcript levels of genes associated with efflux pumps in penicillin-persistent cells of GAS. (b) Influence of CCCP in the expression of genes associated with ABC-type efflux pump (Locus\_tag: MGAS10750\_Spy1817, MGAS10750\_Spy1818, and MGAS10750\_Spy1819) and *ihk/irr* regulators in penicillin-persistent GAS cells; (c) Transcript levels of genes associated with negative transcriptional regulators of efflux pump in penicillin-persistent GAS cells. (d) Transcript levels of genes associated with protein biosynthesis and cell growth in penicillin-persistent GAS cells; (e) Transcript levels of genes associated with stress conditions in penicillin-persistent GAS cells; (f) Transcripts levels of genes associated with toxin-antitoxin (TA) systems in penicillin-persistent GAS cells. Genes locus tag annotated in the genome of the strain MGAS10750 (Acc: NC\_008024) were used as a reference for primer design. a:  $p < 0.05$ ; b:  $p < 0.005$ ; c:  $p < 0.0005$ ; d:  $p < 0.0001$ . For all gene expression assays, the respective calibrator sample (susceptible cells) was assigned relative quantification equal 1. For all tests, JZS Bayes factor agrees with t test, except for the gene locus MGAS10750\_Spy1019 for which the Bayes Factor (BF=1.042144) was in favor of the alternative hypothesis; *bsaA* (BF=1.289759; in favor of alternative hypothesis); *sodA* (BF=1.213086; in favor of the alternative hypothesis); *relB* (BF= 1.349216; in favor of the alternative hypothesis). RQ: Relative quantification.

## Supplementary Files

This is a list of supplementary files associated with this preprint. Click to download.

- [SupplementalTableMartinietal2020.pdf](#)